Modeling the Spread of Epidemic Cholera: an Age-Structured Model

Alen Agheksanterian* Matthias K. Gobbert*

November 20, 2007

Abstract

Occasional outbreaks of cholera epidemics across the world demonstrate that this disease continues to pose a public health threat. Traditional models for the spread of infectious diseases are based on systems of ordinary differential equations. Since the risk for contracting cholera depends on the age of the humans, an age-structured model offers additional insights and the possibility to study the effects of treatment options. The model is given as a system of hyperbolic partial differential equations. We present a finite difference approximation to the model and validate it by studying the effect of high and low rates of shedding of cholera vibrios on the dynamics of the spread of the disease.

Key words. Epidemic cholera, SIR model, Hyperbolic transport, Finite differences.

AMS subject classifications (2000). 92D30, 93A30, 74S20, 81T80.

1 Introduction

The study of cholera continues to be an important problem in mathematical epidemiology, as occasional outbreaks of cholera epidemics continue to pose a public health threat [2], for instance in the environment of a refugee camp with humans in crowded conditions and poor sanitation. A common type of model for the spread of an infectious disease is an SIR model, so named after the categorization of individuals in the classes of susceptible, infected, and removed (recovered) populations. SIR models of cholera developed so far are time dependent models which give rise to a system of ordinary differential equations (ODEs); see [2, 5]. To model the pathway of infection more precisely, authors in [5] proposed a model which takes into account the role of hyper-infective vibrios introduced to the water reserves

*Department of Mathematics and Statistics, University of Maryland, Baltimore County, 1000 Hilltop Circle, Baltimore, MD 21250 {aa5,gobbert}@math.umbc.edu.

by the infected people in the population; this explains the explosive nature of the disease more clearly as seen in historical accounts of cholera epidemics [5].

The next stage in providing a more complete model is taking into account the influence of age of people in the model, because people of different ages have different pathologies of infection. Although using age-structured models to study the spread of infectious diseases is not in itself a new idea (see [1] for example), to the knowledge of these authors no such model has been proposed for the case of cholera. The heart of an age-structured model is a coupled system of hyperbolic partial differential equations (PDEs). The introduction of a system of PDEs instead of a system of ODEs increases the inter-connectivity of the problem greatly; moreover, as we will see in the remaining of this paper, the intricate nature of cholera makes the problem more complicated. The more complicated system of equations turns the numerical computation into a non-trivial task which introduces new challenges not encountered in the traditional ODE models.

This paper is the result of communications with David Hartley [4] (Georgetown University), Holly D. Gaff (Old Dominion University), Elsa Schaefer (Marymount University), Renee Fister (Murray State University), and Glenn Morris (University of Florida). The model presented in this paper is a result of a number of meetings that started from Summer of 2005 and has been through several stages of development. The eventual goal is to at some point combine the model in this paper with an optimal control model to provide a practical method of choosing effective preventive and treatment strategies to minimize the human and material costs incurred in cholera epidemics.

This paper is structured as follows: In Section 2, we will discuss the system of partial differential equations along with initial and boundary conditions that form our SIR model. In Section 3, we discuss the numerical method implemented. Subsequently in Section 4, we discuss the numerical experiments conducted and present our computational results and their practical interpretations. Finally, we finish with concluding remarks in Section 5.

2 The Model

In this section, we describe the system of differential equations which describe our SIR model. We consider a given population, which we divide into three categories: susceptible, infected, and removed (or recovered) populations. We denote the age-density of susceptible, infected, and removed populations by $S = S(a,t)$, $I = I(a,t)$, and $R = R(a,t)$ as functions of age a and time t. With concentration units of humans / week, the number of susceptible people between, for instance, ages a_1 and a_2 at a time t is given by $\int_{a_1}^{a_2} S(a,t)\,da$. We denote the hyperinfective and non-hyperinfective vibrios by $B_H = B_H(t)$ and $B_L = B_L(t)$, respectively. These five quantities, S, I, R, B_L, and B_L, are the dependent variables of the model.

To account for the various factors affecting the dynamics of a cholera epidemic, we have introduced additional coefficient functions, which in most cases vary with age or time (or both). See Table 1 for a complete description of the model quantities and their units.

The system of differential equations in our model is as follows:

$$\begin{aligned}
\frac{\partial S}{\partial t}+\alpha\frac{\partial S}{\partial a} &= \Lambda(a,t)-\beta_L(a)\frac{B_L(t)}{\kappa_L(a)+B_L(t)}S(a,t)-\beta_H(a)\frac{B_H(t)}{\kappa_H(a)+B_H(t)}S(a,t)\\
&\quad -b(a)S(a,t)+\omega(a)R(a,t),\\
\frac{\partial I}{\partial t}+\alpha\frac{\partial I}{\partial a} &= \beta_L(a)\frac{B_L(t)}{\kappa_L(a)+B_L(t)}S(a,t)+\beta_H(a)\frac{B_H(t)}{\kappa_H(a)+B_H(t)}S(a,t)-b(a)I(a,t)\\
&\quad -(1-h(a,t))\Delta(a)I(a,t)-\gamma_1(1-u(a,t))I(a,t)-\gamma_2u(a,t)I(a,t),\\
\frac{\partial R}{\partial t}+\alpha\frac{\partial R}{\partial a} &= \gamma_1(1-u(a,t))I(a,t)+\gamma_2u(a,t)I(a,t)-b(a)R(a,t)-\omega(a)R(a,t),\\
\frac{dB_H}{dt} &= \int_0^A \xi\eta I(a,t)da-\chi B_H(t),\\
\frac{dB_L}{dt} &= \chi B_H(t)-\delta_L B_L(t).
\end{aligned}$$

In the above equations, $\alpha = 1/7$ week / days is a coefficient introduced to balance the units of age a in weeks and time t in days. Also, A which appears in the equation for B_H is an upper bound on age of people in the model (we used $A = 72$ years is our simulations).

2.1 The Boundary Conditions

The boundary conditions for S, I, and R are determined by the following assumptions:

- Newborns are not susceptible.
- Newborns are not infected with cholera.
- Initially all births are protected.

The above assumptions which are based on the nature of cholera say that in the first place, cholera does not transmit vertically (an infected mother cannot give the disease to a newborn infant); moreover, new born babies have in fact some immunity toward the disease which they loose over time (with a given waning rate). We note that the immunity against infection at time of birth makes this model different from other age-structured SIR models of infectious diseases.

The above considerations translate to the boundary conditions

$$\begin{aligned}
S(0,t) &= 0,\\
I(0,t) &= 0,\\
R(0,t) &= \int_0^A (S(a,t)+I(a,t)+R(a,t))f(a)da,
\end{aligned}$$

where the fecundity function f is modeled as

$$f(a)=\begin{cases}\frac{1}{5}\sin^2\left[\left(\frac{a-15}{30}\right)\pi\right], & 15<a<45,\\ 0, & \text{otherwise.}\end{cases} \tag{2.1}$$

This fecundity function is stated here in units of 1 / years for easier readability and assumes that from age 15 to 45 years a woman will generally give birth to three children, since

$$\int_0^A f(a)\,da = 3, \tag{2.2}$$

where A is the largest age allowed in the model.

2.2 The Initial Conditions

To keep the formulation general, we leave the initial condition functions

$$\begin{aligned} S(a,0) &= S_0(a), \\ I(a,0) &= I_0(a), \\ R(a,0) &= R_0(a), \\ B_L(0) &= B_{L0}, \\ B_H(0) &= B_{H0}. \end{aligned}$$

to be specified below. In the subsequent sections, where we discuss computational details, we will list the actual functions used in computations.

2.3 Model Parameters and Their Units

As the reader can see, the differential equations describing our model incorporate various biological and demographic effects into consideration. Here we have listed all model parameters with brief descriptions in Table 1. To make things clear, we have also stated the units for each of the quantities.

2.4 Choice of Units for Age a and Time t

In a theoretical discussion, units of variables in equations are not so important because one knows that everything can be balanced with a suitable coefficient. However, while doing computations on concrete problems one needs to pay close attention to the units of the model quantities. To make a dimensional study of the model simpler, we chose units of weeks for the age of humans a and days for the simulation time t. This is to avoid confusions which may arise if one decides to have the same units for both a and t.

Quantity	Description	Units
a	age	weeks
t	time	days
$S(a,t)$	susceptible humans of age a at time t divided uniformly over all ages	$\frac{\text{human}}{\text{week}}$
$I(a,t)$	infected and infectious humans of age a at time t	$\frac{\text{human}}{\text{week}}$
$R(a,t)$	removed and immune humans of age a at time t	$\frac{\text{human}}{\text{week}}$
$B_H(t)$	HI vibrio population	cells/ml
$B_L(t)$	non-HI vibrio population	cells/ml
α	proportionality factor (wave speed)	week / days
$\Lambda(a,t)$	recruitment rate, number of susceptible humans entering population of age a at time t	$\frac{\text{human}}{\text{week}-\text{day}}$
$h(a,t)$	oral rehydration therapy, reduces disease related mortality (90% effective)	none
$u(a,t)$	antibiotic treatment rate for humans of age a at time t	none
$\beta_L(a)$	ingestion rate of non-HI vibrios	/day
$\beta_H(a)$	ingestion rate of HI vibrios	/day
$\kappa_L(a)$	saturation constant of non-HI vibrios	cells/ml
$\kappa_H(a)$	saturation constant of HI vibrios	cells/ml
$b(a)$	natural mortality rate of humans at age a	/day
$\omega(a)$	rate of waning immunity of humans at age a	/day
$\Delta(a)$	disease related mortality rate for humans at age a	/day
$f(a)$	maternity rate	/week
γ_1	recovery rate of untreated cholera	/day
γ_2	recovery rate of treated cholera	/day
ξ	rate of shedding of cholera vibrios from infected human of age a	$\frac{\text{cells}}{\text{ml}-\text{day}-\text{human}}$
η	relative amount of stool per time	(no dimension)
χ	rate of vibrio moving from HI to non-HI state	/day
δ_L	death rate of vibrio in the environment	/day

Table 1: Model parameters and their units (HI = hyperinfective).

3 Numerical Method Implemented

In this section, we describe briefly the numerical method used in our computations. The equations for the quantities S, I, and R form a hyperbolic system of PDEs; coupled with these, we have the two ODEs for B_H and B_L. Our choice of numerical method is a forward time/backward space finite difference scheme [6]. For the convenience of the reader we recall the scheme for the simpler case of the scalar one-way wave equation

$$\frac{\partial u}{\partial t} + \alpha \frac{\partial u}{\partial x} = f(x,t). \tag{3.1}$$

where α is a constant (physically the wave speed), and t and x represent time and space, respectively. The forward time/backward space scheme [6] for the above problem is given by

$$\frac{u_m^{n+1} - u_m^n}{\Delta t} - a\frac{u_m^n - u_{m-1}^n}{\Delta x} = f(x_m, t_n),$$

where n denotes the time index and m the space index in the time and space grid.

We also recall that any explicit scheme is only conditionally stable [6]. To ensure stability of the scheme, a necessary and sufficient condition is the famous Courant-Friedrichs-Lewy (CFL) condition (Theorem 1.6.1 in [6]) which requires

$$\left| \alpha \frac{\Delta t}{\Delta x} \right| \leq 1. \tag{3.2}$$

For a given spatial discretization Δx, this yields a restriction on the time step as $\Delta t \leq \Delta x/|\alpha|$.

4 Computational Experiments and Results

In this section, we present three simulations to test robustness and accuracy of our model. However, we point out that the model parameters, especially the age dependent coefficient functions, require more careful research and hence, at this point, our current results are mainly useful in a qualitative sense. Nevertheless, even qualitative information on the dynamics of a disease as complicated as cholera can be helpful in gaining further insight.

4.1 The Reference Simulation with No Infected Population

Suppose we have a pool of 10,000 humans distributed uniformly over the age range $0 \leq a \leq A$, none of whom are infected. We assume that initially no one is in the removed (recovered) category, and so we let $R(a,0) = 0$ for all a. Therefore, in this case we will have the whole initial population as susceptible which translates to $\int_0^A S(a,0)\,da = 10{,}000$. For the initial non-hyperinfective and hyperinfective vibrio populations we make the following assumptions: $B_L(0) = 0$, $B_H(0) = 0$. These assumptions fix the choice of initial conditions in our system

Quantity	Value
$\Lambda(a,t)$	0
$h(a,t)$	0.9
β_L	$\frac{1.5}{7}$
β_H	$\frac{1.5}{7}$
κ_L	10^6
κ_H	$\frac{\kappa_L}{700}$
γ_1	$\frac{1}{5}$
γ_2	$\frac{1}{3}$
ξ	10^9
η	0.1
χ	$5/hour$
δ_L	$\frac{1}{30}$

Table 2: Values of the model parameters in all simulations except ξ in Section 4.3

of differential equations. The rest of the model parameters, which are mostly taken from [4], are specified below.

The rate of waning of immunity of humans at age a is modeled by [4]

$$\omega(a) = \begin{cases} 1/(2 \cdot 365), & a > 10 \text{ years old}, \\ 1/365, & a \leq 10 \text{ years old}. \end{cases}$$

To model the disease related mortality rate, we use [4]

$$\Delta(a) = \begin{cases} 0.007, & a > 10 \text{ years old}, \\ 0.032, & a \leq 10 \text{ years old}. \end{cases}$$

Table 2 lists the values for the remaining model parameters.

With no infected people in the initial population, we expect the number of sick people remain at zero. Thus, our model effectively becomes a population model. However, we still get some useful information from this simulation. In Figure 1, we depict the dynamics in the total population, susceptible population, infected population, and removed (recovered) population over time. Note that in this case, we see an increase in total population which is merely due to the positive balance in the rate at which babies are born versus natural death rate of people. We note here the decrease in the susceptible population, which is due to people who died of natural causes during the time-line of the simulation. Moreover, we see an increase in removed (recovered) population, which is due to the fact that newly born infants have immunity toward cholera, and it takes some time until they lose their immunity (which is governed by the rate of waning of immunity).

4.2 Spread of an Epidemic with High Rate of Shedding of Cholera

Again, we start with an initial population of 10,000 people, and as before we let $R(a,0) = 0$ for all ages a. However, this time we will put one infected person in the initial population.

In this simulation, the infected population is distributed over the numerical grid such that

$$\int_{18}^{19} I(a,0)\,da = 1,$$

where we have used units of years for easier readability. Note that the above initial condition on I can be interpreted as having one infected person of age 18 in the initial population. Finally, the rest of the population is assumed to be in the susceptible category, that is we require $\int_0^A S(a,0)\,da = 9{,}999$, so that the total population adds up to 10,000 humans. The model parameters are listed in Table 2. As before, the plots in Figure 2 depict the total population over time, the susceptible population over time, the infected population over time, and the removed (recovered) population over time. We note the explosive nature of the spread of cholera in the plot of infected people where we see a high of about 5,000 sick people within the first couple of weeks of the epidemic. Qualitatively similar results were obtained in [5] using an ODE model. We also looked at the dynamics of B_H and B_L over time which are depicted in Figures 3 (a) and (b), respectively. Now to take advantage of our PDE model, we can look at the model quantities over all ages and all times in Figure 4 which show how the quantities change over time across different age groups. For example, in Figure 4, in the surface plot of the susceptible population, the height (the vertical coordinate) at point (a,t) is the number of susceptible people of age a at time t.

4.3 Spread of an Epidemic with Low Rate of Shedding of Cholera

In the previous simulation, we noted that our model reports a total of 5,000 sick people in less than two weeks; this points out the explosive nature of cholera as seen in real world [3]. One may simply ask, which aspect of the model captures this explosive nature of cholera. The answer to that question lies in the role played by hyperinfective vibrios $B_H(t)$ [5]. Recall that in the system of differential equations describing our model, we had the ODE

$$\frac{dB_H}{dt} = \int_0^A \xi\eta I(a,t)da - \chi B_H(t), \tag{4.1}$$

where ξ is the rate at which infected people shed hyperinfective vibrios into the aquatic environment. In the previous simulations, we had $\xi = 10^9$. Making this number smaller implies that less hyperinfective agents are being released by people. To see what will happen in this case, we conducted our third simulation, where we let $\xi = 10^2$. The remaining parameters are as listed in Table 2.

The results of this simulation reported in Figures 5, 6, and 7 show the dynamics of the epidemic in this case of lower rate of shedding of cholera. We see that when the hyperinfective vibrios play a less significant role, the result is a milder breakout of the disease. We see here that we get less than 1,500 infected people in over six weeks time, which is a much less severe case than that of our previous simulation.

5 Discussion

An age-structured model can model the infection pathway of cholera more precisely, since the risk for contracting the disease depends on the age of a human. We see that introducing age as another independent variable entails solving a system of partial differential equations instead of simpler ODE systems; this introduces new challenges for the numerical method. The reference simulation without any infected population reproduces the behavior of a population model. A simulation with a high rate of shedding of cholera produces results that show the same rapid speed of infection as traditional ODE models. To test the fidelity of the model and its implementation, a simulation with a low rate of shedding of cholera is contrasted, which has a more moderate spike of infections. This shows the central role played by the hyperinfective vibrios shed by infected and infectious people in the population, an important element pointed out in [5]. Other terms in the equations model the effect of several treatment options. The results obtained by varying the rate of shedding motivate that also studies on the treatment options should be possible with this age-structured model and its implementation.

References

[1] L. J. Allen, *An Introduction to Mathematical Biology*, Prentice-Hall, 2006.

[2] C. T. Codeço, *Endemic and epidemic dynamics of cholera: the role of the aquatic reservoir*, BMC Infect Dis., 1 (2001).

[3] ——, *Trends in cholera epidemiology*, PLoS Med., 3 (2006).

[4] D. Hartley, *personal communications*, 2006.

[5] D. M. Hartley, J. G. Morris, and D. L. Smith, *Hyperinfectivity: A critical element in the ability of v. cholerae to cause epidemics?*, PLoS Med., 3 (2006).

[6] J. Strikwerda, *Finite Difference Schemes and Partial Differential Equations*, SIAM, second ed., 2004.

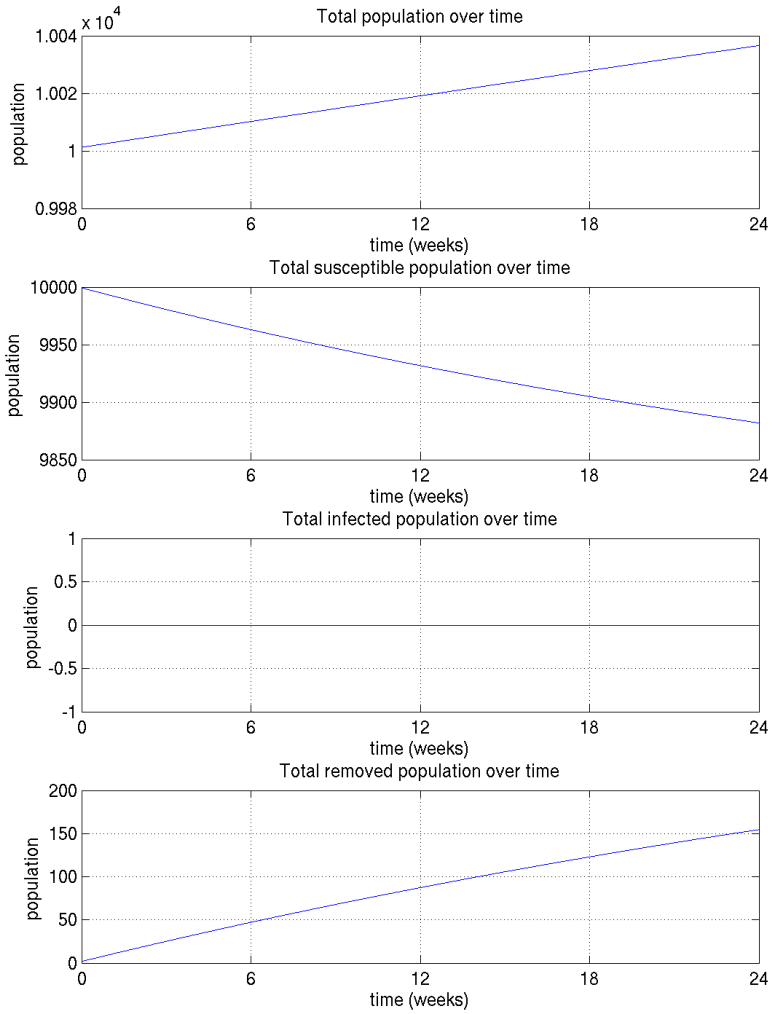

Figure 1: Reference simulation with no infected population: dynamics of the cholera epidemic over time.

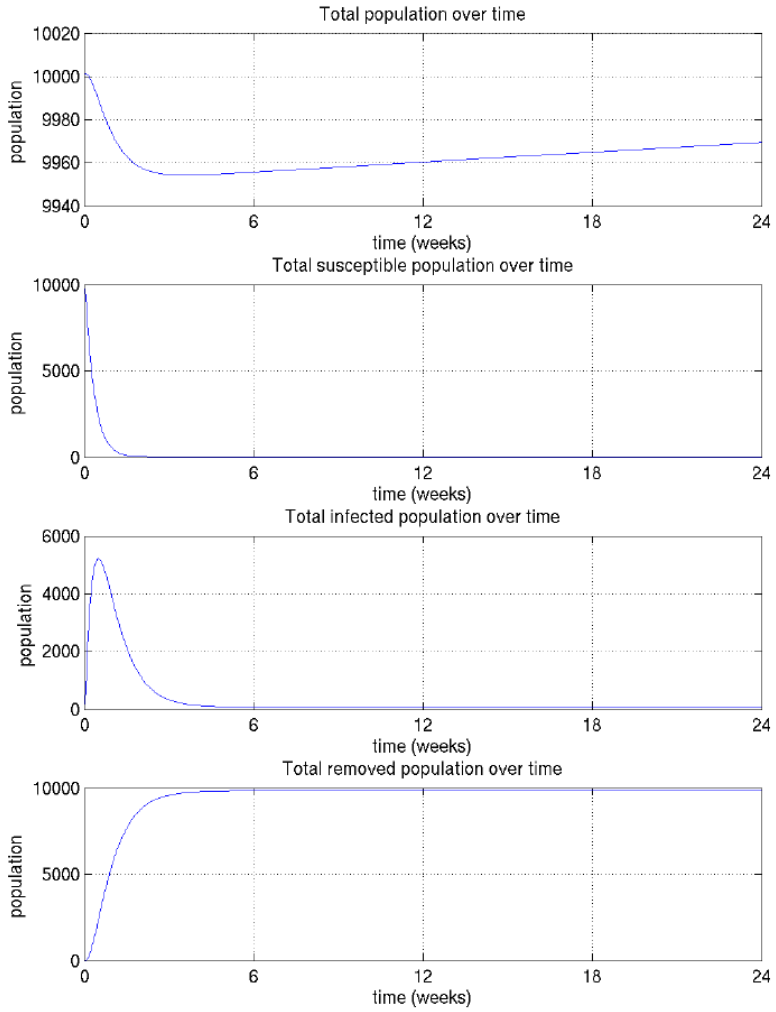

Figure 2: High rate of shedding of cholera: dynamics of the cholera epidemic over time.

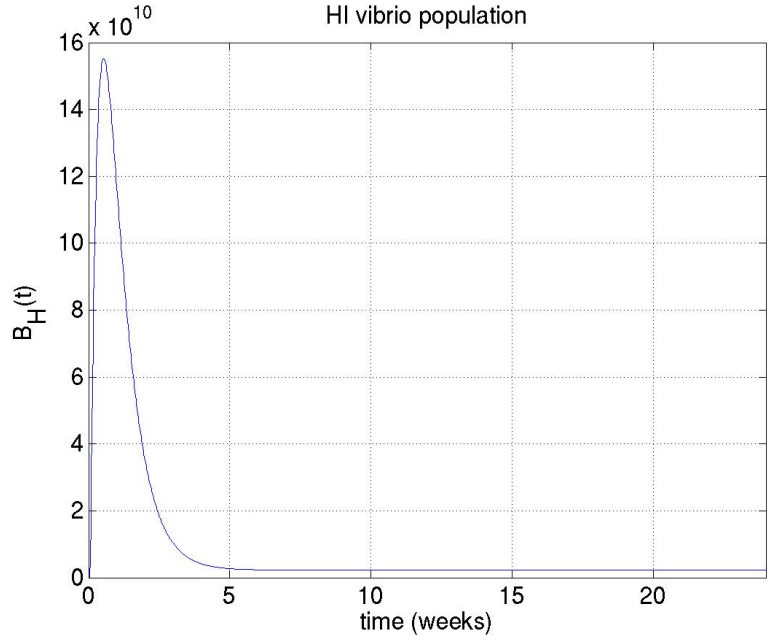

(a)

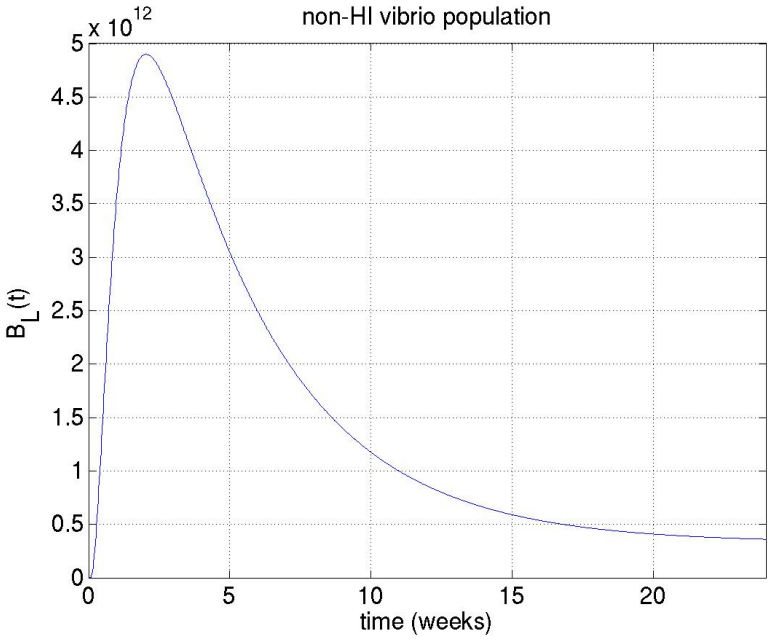

(b)

Figure 3: High rate of shedding of cholera: (a) B_H over time, (b) B_L over time.

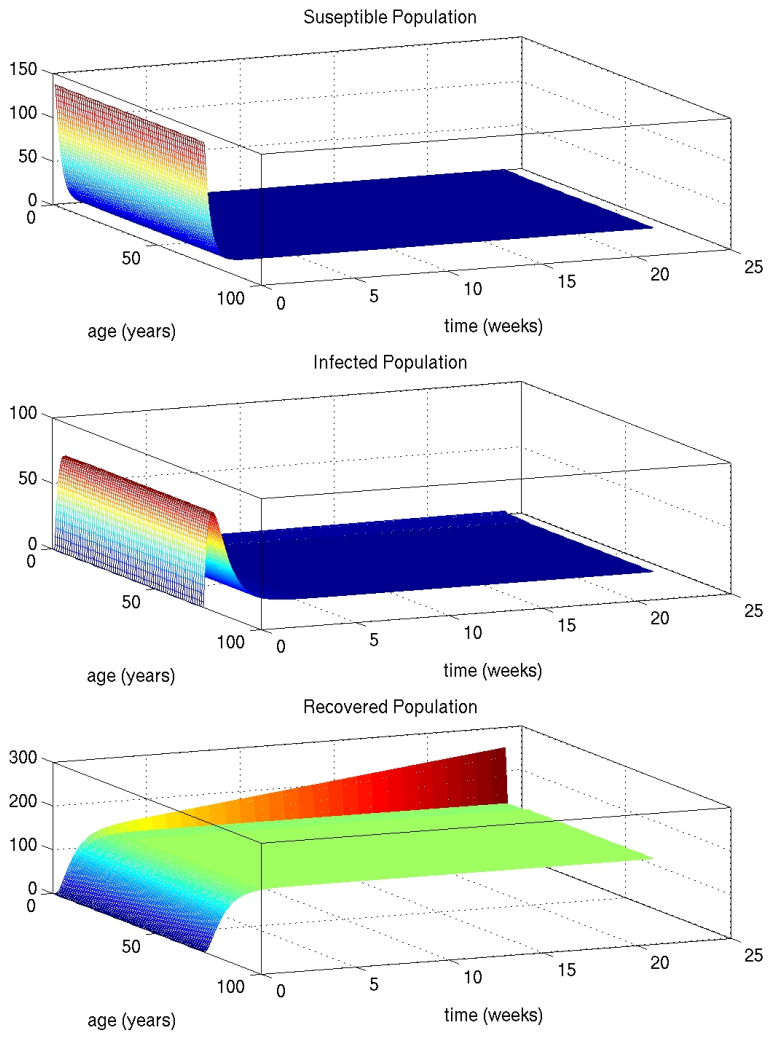

Figure 4: High rate of shedding of cholera: dynamics of the cholera epidemic as function of age and time.

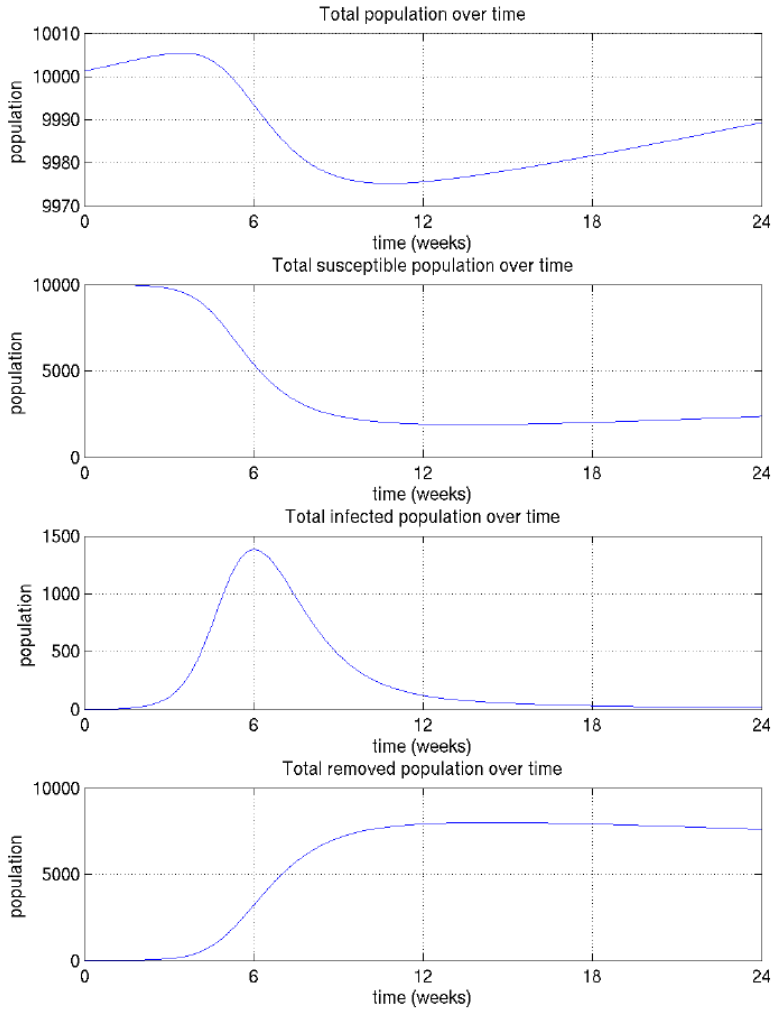

Figure 5: Low rate of shedding of cholera: dynamics of the cholera epidemic over time.

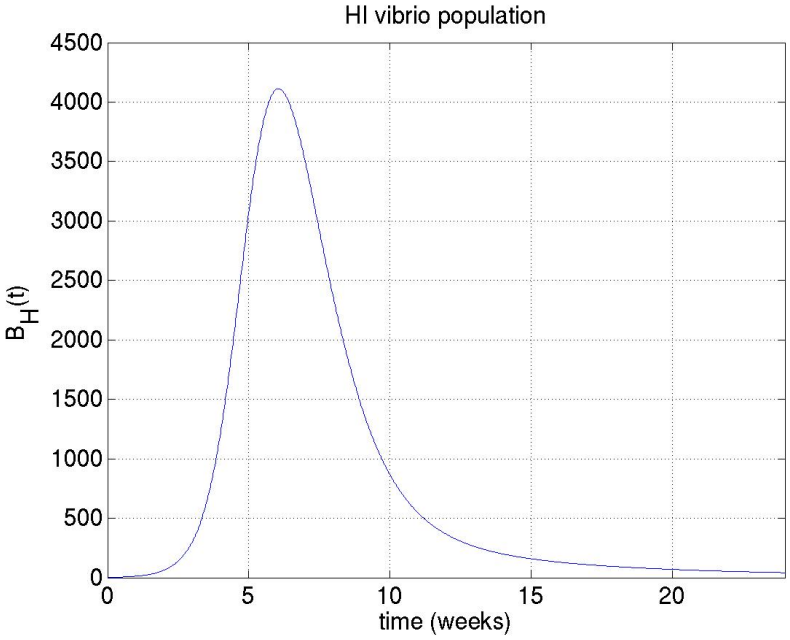

(a)

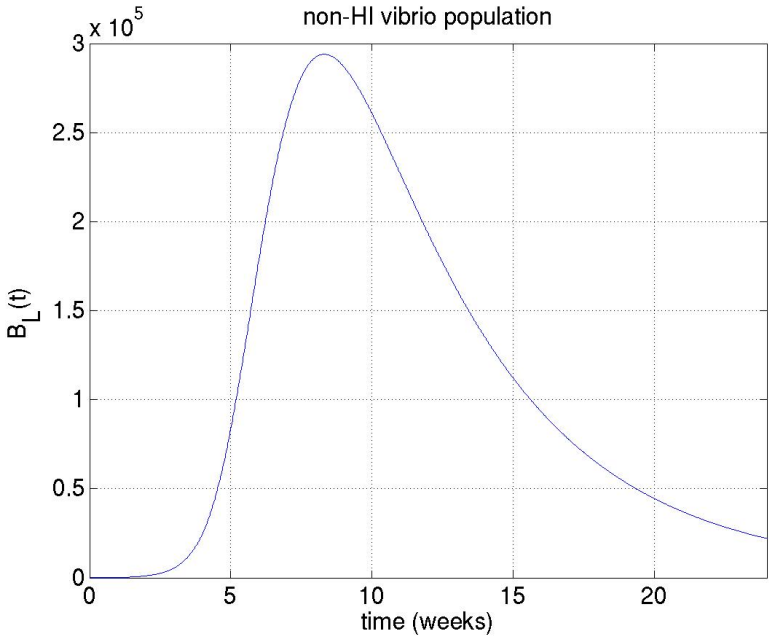

(b)

Figure 6: Low rate of shedding of cholera: (a) B_H over time, (b) B_L over time.

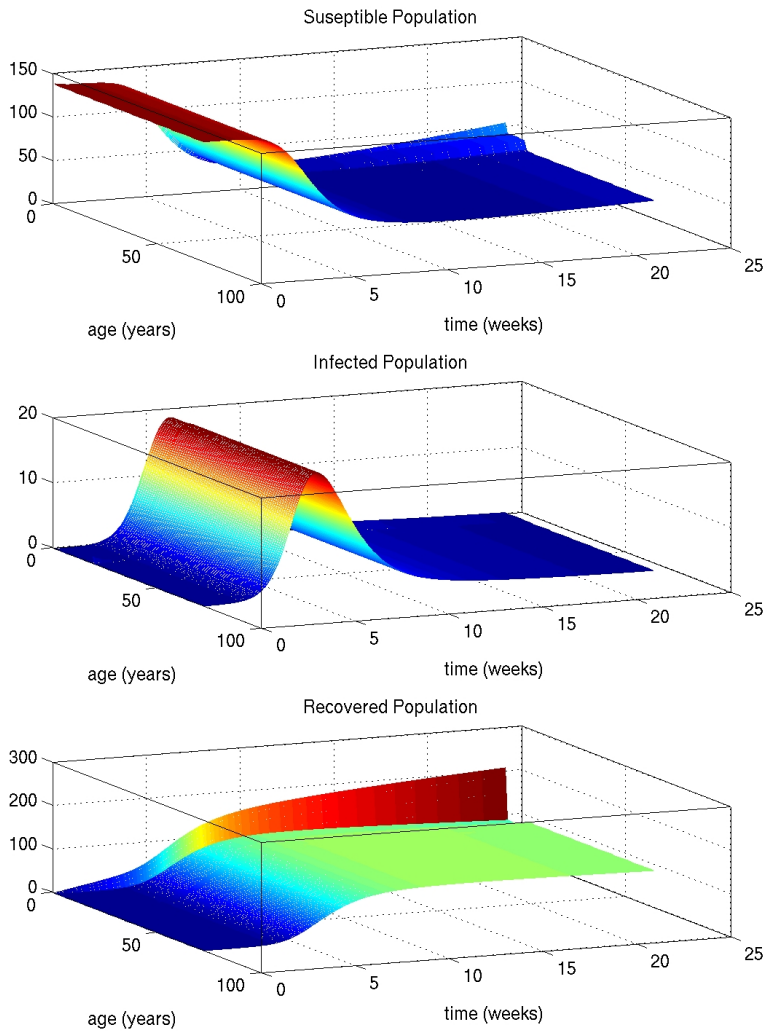

Figure 7: Low rate of shedding of cholera: dynamics of the cholera epidemic as function of age and time.